Calibration and Testing of a Water Model for Simulation of the Molecular Dynamics of Proteins and Nucleic Acids in Solution

Michael Levitt*

Beckman Laboratory for Structural Biology, Department of Structural Biology, Stanford School of Medicine, Stanford, California 94305

Miriam Hirshberg

Protein Structure Group, National Institute for Medical Research, The Ridgeway, Mill Hill, London NW7 1AA, U.K.

Ruth Sharon

Department of Structural Biology, Weizmann Institute of Science, Rehovot, 7600, Israel

Keith E. Laidig and Valerie Daggett*

Department of Medicinal Chemistry, University of Washington, Seattle, Washington 98195-7610

Received: December 9, 1996; In Final Form: April 3, 1997[⊗]

The objective of this work is to obtain a water model for simulations of biological macromolecules in solution. A pragmatic approach is taken in which we use the same type of force field for the water as used for the solute and derive the water potential as an integral part of the ENCAD macromolecular potential.[1,2] Here we describe a flexible three-centered water model (F3C), which has already been used for many large-scale biological simulations, and compare it with other water models. The model is further tested by comparing calculated energetic, structural, and dynamic properties of liquid water, at several temperatures and pressures, with experiment. The F3C model is extremely simple and fits experimental data well for different temperatures, pressures, system sizes, and integration time steps. Because the F3C model works well with short-range truncation, it is well-suited to high-speed computation of long molecular dynamics trajectories of macromolecules in solution.

Introduction

Liquid water is the universal solvent in biological systems. Biological macromolecules, such as proteins and nucleic acids, adopt their structures and carry out their catalytic roles while interacting with thousands of surrounding water molecules. Water enables ionizable groups to retain net charges and is often an intermediary in substrate binding and catalysis. Our focus is on the development and use of computer simulation methods to investigate complicated biological phenomena. Earlier studies have demonstrated that one achieves much more realistic dynamic behavior of proteins when simulations include water molecules explicitly, as opposed to continuum dielectric screening terms.[3,4] Consequently, we have undertaken the development of a simple, robust, and realistic model of water for use in computer simulation of macromolecules in aqueous solutions under a variety of conditions.

Our primary selection criterion for an appropriate water model is that it have the same degrees of freedom and employ the same potential form as used for the macromolecule. Without such an underlying consistency, unexpected and undetected systematic errors could be introduced into the simulations. The need for such coherence was first emphasized by Lifson in the consistent force field used for small organic molecules,[5] and this is even more important in biological macromolecules, where fewer experimental results are available for calibration. Our macromolecular potential function and methods, which have been developed over the last 25 years,[1,6,7] have been presented in full detail elsewhere.[2] The water model presented here is extremely simple, using only the atoms as interaction centers, avoiding any constraints on bond lengths or bond angles, and using potentials that are completely transferable to macromolecules.

Early emphasis on analytical treatments of water was redirected to computer simulation by Rahman and Stillinger's pioneering simulation of liquid water done over 25 years ago.[8] That work, which has served as a prototype for hundreds of subsequent studies, is characterized by (a) use of molecular dynamics of a simple water model to simulate a trajectory (in their case, lasting only 2 ps), (b) comprehensive analysis of the trajectory to extract a wide range of energetic, structural, and dynamic properties, (c) careful comparison of these properties to experiment with the aim of improving the molecular representation of water, and (d) relation of the simulation back to theory and simple conceptual models.

As more work has been done on models of liquid water, the representations of water interactions have developed in two directions. On the one hand, the simple pairwise van der Waals and Coulombic interactions between atom centers and lone-pairs used in Rahman and Stillinger's work have been extended to models that incorporate polarization.[9−20] But, one confronts problems using the more complicated water models together with simple potentials that do not include lone-pairs and polarization necessary for the macromolecules. Having ad-

* Address correspondence to either author.
[⊗] Abstract published in *Advance ACS Abstracts,* June 1, 1997.

S1089-5647(96)04020-5 CCC: $14.00

ditional interaction centers on the water atoms and not on the solute atoms can influence the strength of hydrogen bonds. For example, in an early study of a dipeptide in solution[21] such a mixed representation was used, but solute−water hydrogen bonds had to be treated by a further, special function different from that used for water−water hydrogen bonds.

On the other hand, simpler water models that use fewer interaction centers have been tested[22,23] and found to work as well as the more complicated models. Generally, macromolecular simulations including explicit solvent employ either the SPC[21] or TIP3P[22] model. These simple models have much in common; they both use similar atomic partial changes on the oxygen and hydrogen atoms, which are chosen to give an electrically neutral molecule (Table 1). They also use van der Waals interactions that act only between the oxygen atoms. These features are perfectly matched to protein energy calculations, which generally use nonbonded potentials derived by Lifson and co-workers from molecular crystals.[24−26] In fact, in their study of amide crystals, Hagler et al.[26] showed that the fit to experiment is better without off-atom interaction centers or van der Waals interactions between polar hydrogen atoms. In the simulation of macromolecules, generally the solute is allowed to have flexible bonds and angles, whereas both the SPC and TIP3P models use rigid geometries with fixed bond lengths and angles.

Although both the SPC and TIP3P potentials have been widely used in simulations of different systems including macromolecules in crystals and solution, both models have been further modified to address shortcomings. The TIP3P potential was supplanted by a four-point water model (TIP4P) with an additional negative interaction center off of the oxygen atom.[27] The change to a more complicated model was prompted by the lack of tetrahedral water structure in TIP3P (Table 2). This structure, quantified by the height of the second peak in the oxygen−oxygen radial distribution function, is thought to be responsible for the unusual room-temperature properties of liquid water. In addition to their supposed lack of tetrahedral structure, these simple water models did not reproduce the transport properties of water, giving a diffusion constant that is too high at room temperature (Table 2). This led to a reparametrization of the SPC model to give the SPC/E model,[28] in which the diffusion rate is reduced at the expense of making the heat of vaporization even more negative than the experimental value (Table 2) (the difference is justified in terms of the neglected energy required to polarize a real water molecule as it goes from vapor to liquid).

Given that in our treatments of protein dynamics we have always allowed all degrees of freedom,[1] we are interested in flexible water molecules. Some previous water models have also allowed the OH bond lengths and HOH bond angles to vibrate, making it pertinent to ask whether such additional flexibility changed the calculated properties. Stillinger and Rahman[29] introduced a novel flexible water model that allowed hydrogen atoms to dissociate in the liquid. The model reproduced water structure but gave too small a diffusion rate. Several studies of flexible three-point water models using either the SPC[30−33] or TIP3P[34] parametrizations found that flexibility did not increase tetrahedral structure, while in other simulations flexibility did lead to more tetrahedral structure.[3,35] The diffusive properties of water also seem to depend on the internal flexibility, but there is disagreement about whether flexibility increases[31] or decreases[3,36,37] the diffusion constant. Although rigid water is still used most commonly in simulations of macromolecules, an increasing number of recent simulations do include internal flexibility.[15,38−44]

TABLE 1: Energy Parameters[a] of Three-Point Water Models

parameters and units	TIP3P	SPC	F3C
r_0^{OO} (Å)	3.5365	3.5532	3.5532
ϵ^{OO} (kcal mol^{-1})	0.1521	0.1554	0.1848
A^{OO} (kcal Å^{12} mol^{-1})	582 000	629 400	748 407
B^{OO} (kcal Å^6 mol^{-1})	−595.0	−625.5	−743.8
r_0^{HH} (Å)	0	0	0.9000
ϵ^{HH} (kcal mol^{-1})	0	0	0.01
A^{HH} (kcal Å^{12} mol^{-1})[b]	0	0	0.0028
B^{HH} (kcal Å^6 mol^{-1})[b]	0	0	0.0106
q^O (e units)	−0.834	−0.820	−0.820
q^H (e units)	0.417	0.410	0.410
b_0^{OH} (Å)	0.9572	1.0000	1.0000
θ_0^{HOH} (deg)	104.52	109.47	109.47
K_b^{OH} (kcal mol^{-1} Å^{-2})[c]			250
K_θ^{HOH} (kcal mol^{-1} rad^{-2})			60

[a] The complete form of the energy function used here for water is

$$U = \sum_{\text{bond lengths}} K_b(b_i - b_0)^2 + \sum_{\text{bond angles}} K_\theta(\theta_i - \theta_0)^2 + \sum_{\text{nonbonded pairs } i,j \text{ closer than cutoff}} [A_{sc}\epsilon(r_0/r_{ij})^{12} - 2\epsilon(r_0/r_{ij})^6 - S_{vdw}(r_{ij})] + \sum [q^i q^j/r_{ij} - S_{els}(r_{ij})]$$

where the energy parameters (K_b, b_0, K_θ, θ_0, ϵ, r_0, and q^i) are given above for the different atom types. The variables calculated from the atomic Cartesian coordinates are b_i, the bond length, θ_i, the bond angle, and r_{ij}, the interatomic distance. The truncation shift function, $S_f(r)$, which has the general form

$$S_f(r) = [f(r_c) + (r - r_c)(df(r_c)/dr)] \quad \text{for} \quad r < r_c$$

$$= 0 \quad \text{for} \quad r \geq r_c$$

the energy function, $f(r)$, is different for van der Waals and electrostatic terms:

$$S_{vdw}(r) = [A_{sc}\epsilon(r_0/r_c)^{12} - 2\epsilon(r_0/r_c)^6] - 12(r - r_c)[A_{sc}\epsilon(r_0/r_c)^{12} - \epsilon(r_0/r_c)^6]/r_c$$

$$S_{els}(r) = [q^i q^j/r_c] - (r - r_c)[q^i q^j/r_c^2]$$

where r_c is the cutoff distance. The A-scale parameter, A_{sc}, reduces the repulsive van der Waals energy to compensate for attractive interactions lost by smaller cutoff distances. In the ENCAD program, pairs of nonbonded distances are collected to a range that is 2 Å larger than the cutoff, r_c, and then used for 2−5 iterations. [b] The repulsive parameter, A, is calculated as ϵr_0^{12}, and the attractive parameter, B, as $-2\epsilon r_0^6$. The values of ϵ and r_0 used for a particular atom pair are the geometric means of the tabulated values, whether water−water or macromolecule−water interactions are considered, as described elsewhere.[2] [c] The K_b^{OH} value of 250 kcal mol^{-1} Å^2 used here is about half that used in other flexible water models (for example, $K_b^{OH} = 553$ kcal mol^{-1} Å^2 in AMBER[75] and 450 kcal mol^{-1} Å^2 in CHARMM[76]). Our K_θ^{HOH} value of 60 kcal mol^{-1} rad^2 is similar to others (55 kcal mol^{-1} rad^2 in AMBER and 47 kcal mol^{-1} rad^2 in CHARMM).

Given that molecular dynamics simulations of macromolecules in solution are more accurate than those *in vacuo*[3,4] and that simpler water models are more efficient computationally, allowing longer simulations of large systems, we have chosen to develop a water model with full flexibility, energy conservation, and smooth atom-based truncation to give a simple three-point model, coined F3C. Here we present this water model and rigorously evaluate it under a variety of solution conditions. First, we compare the general features of our water model to other models and to experiment. We then investigate how properties calculated from the model fit experiment as a function of temperature and pressure. Next, we show the effect

TABLE 2: Comparison of Properties[a] of the F3C Model and Other Water Models with Experiment

model			thermodynamic			kinetic	structural					
							g_{OO} heights			positions (Å)		
name	date	n_{cen}[b]	T (K)	U_{pot} (kcal mol^{-1})	C_V (cal mol^{-1} K^{-1})	$D \times 10^4$ (cm^2 s^{-1})	gp1	gv1	gp2	Rp1	Rv1	Rp2
F3C[c]		3	298	−9.6	26(20)	0.24	3.19	0.83	1.07	2.8	3.3	4.4
(σ)[c]			(5)	(0.05)	(1.6)	(0.023)	(0.25)	(0.02)	(0.01)	(0.0)	(0.0)	(0.1)
expt			298	−9.9	18	0.23	2.91	0.73	1.14	2.9	3.3	4.5
Other Three-Point Models												
RCF	1978[29]	3	302	−9.5		0.11	3.1	0.64	1.15	2.8	3.3	4.5
TIP3P	1980[23,27]	3	298	−9.9	17	0.40	2.9			2.8		
SPC	1981[22,27]	3	298	−10.2	23	0.36	2.8	0.90	1.05	2.8	3.3	4.5
SPCE	1987[28]	3	300	−10.8		0.25	3.0	0.80	1.10	2.7	3.3	4.7
Multicenter Models												
BF	1933[27,77]	4	298	−10.5	18	0.43	2.7	0.80	1.10	2.9	4.7	6.0
BNS	1971[8,78]	5	308	−9.2		0.42	2.6	0.64	1.26	2.7	3.4	4.7
ST2	1974[8,79]	5	283	−10.4	22	0.19	3.2	0.68	1.18	2.8	3.5	4.7
ST2	1974[8,79]	5	314	−9.8		0.43	3.0	0.75	1.08	2.9	3.5	4.7
MCY	1976[70,80,81]	4	294	−8.6		0.23	3.4	0.90	1.11	2.8	2.5	4.2
TIP4P	1983[27,82]	4	298	−10.1	19	0.32	3.0	0.81	1.12	2.8	3.4	4.5
Polarizable Model												
PSPC	1988[12,17,19]		300	−9.1		0.24	2.4			2.8		
DCS	1988[10]	7	300	−9.9			3.6	0.65	1.15	2.8	3.3	4.5
NEMO	1990[14,17]		300	−9.6		0.08	3.1	0.65	1.22	2.8	3.3	4.3
POL1	1990[13,18]		303	−9.9			2.9	0.82	1.10	2.8	3.3	4.3
FPW	1991[16]		298	−9.6		0.16	3.4	0.70	1.00	2.9	3.2	4.0

[a] Key to properties that are calculated as time averages from the simulation (references are to the source of experimental values): T, temperature calculated from the kinetic energy (K); U_{pot}, potential energy per water molecule (kcal/mol);[54] C_V, heat capacity calculated from the fluctuation of the kinetic energy (cal/(mol K));[48] the value given in parentheses for the F3C model is after correction for the quantization of high-frequency vibrations;[54] D, diffusion constant calculated from mean square oxygen displacement (cm^2/s);[56] gp1, gv1, & gp2, heights of first peak, first valley, and second peak in the O···O radial distribution function;[61] Rp1, Rv1, & Rp2, position (in Å) of these three features, respectively.[61] [b] n_{cen} is the number of interaction centers in the model (if greater than 3, there are additional centers representing "lone-pair" interaction centers). [c] The F3C entry gives the average and standard deviation of six independent 100 ps runs at the same target temperature of 298 K. These standard deviations are a good estimate of the errors for all runs presented here. The F3C entry is for an 8 Å range ($r_c = 6$ Å).

of varying system sizes, integration time steps, and nonbonded interaction ranges. And finally, we address the electrostatic screening properties of the model.

Methods

The F3C water model is specifically designed for use in simulations of macromolecules. As such, it has to meet two design criteria: that it use consistent potentials for all interactions and that it conserve energy with a short-range cutoff.

Consistency, which is based on ideas pioneered by Lifson and co-workers,[23−25] requires that the form of the potential for water and macromolecules be the same. In other words, one should not use additional lone-pairs in the water nor omit any atoms in the macromolecule (such as the nonpolar hydrogen atoms), and if bond lengths and angles are flexible in the macromolecule, they cannot be fixed in water. In F3C we use all atoms as interaction centers but do not include any additional centers, as is done for the macromolecule.[2] We also allow flexibility of all bond lengths and bond angles both in the water and in the macromolecule. Parameters for the water interaction are given in Table 1, except where modified for testing purposes, as described in the text, and the complete set of energy parameters for macromolecules is given elsewhere.[2] In contrast to other flexible water models derived from the SPC model, the OH bond and HOH bond angle adopt the same parameters used for these interactions in the macromolecule.

We choose to use the NVE (microcanonical) ensemble for our simulations, which fixes the number of particles, conserves energy and keeps volume constant. In order to achieve the desired energy conservation, the integration of the equations of motion must keep errors to a minimum. In particular, the energy function and forces (first derivatives) should be continuous functions of the atomic positions. One source of discontinuity comes from ignoring interactions between atoms that are further apart than some cutoff distance. While such truncation of long-range interactions can save a great deal of computation in simulations that include thousands of polypeptide and/or polynucleotide atoms and water molecules, achieving energy conservation with truncation is not a trivial matter.[2,45,46] We have developed and tested schemes for ensuring smooth truncation of the energy and minimizing spurious forces.[2] The smoothing functions used are given in Table 1.

The simulation protocols,[47,48] as implemented within ENCAD,[49] have been described. The equations of motion were integrated using a modified version of the Beeman method, as described by Levitt et al.[2] A cubic water box with 216 water molecules was used. The density of the solvent was set to the experimental value for the temperature of interest[50,51] (273−573 K) by adjusting the volume of the box. Minimum image conditions[48] were used, and since solvent molecules were explicitly present, no macroscopic dielectric constant was needed. The resulting systems were then prepared for molecular dynamics with a total of 2000 cycles of conjugate gradient minimization performed on the entire system. Atoms in the system were randomly assigned velocities appropriate for the temperature of the simulation according to a Maxwellian distribution. Atoms were allowed to move according to Newton's equations of motion, and the velocities of the atoms were adjusted intermittently until the system reached the desired temperature. After the temperature was reached, no further velocity scaling was needed and the total energy of the system remained constant, with a rmsd of less than 0.1%. A 2 fs (1 fs = 10^{-15} s) time step was used for both the preparation and the full simulation of 100 ps (1×10^5 steps), except during the test of time step dependence (*vide infra*). Each property is calculated by averaging over all water molecules in the box during the last 50 ps of each 100 ps

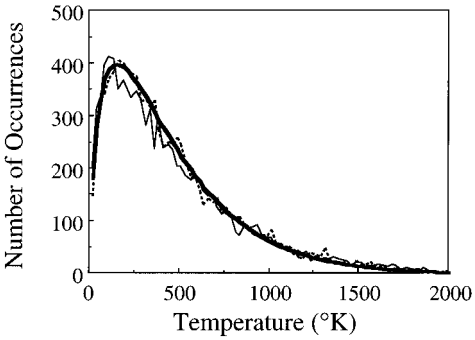

Figure 1. Distribution of temperature values (calculated from kinetic energy) of (a) all water atoms collected over a very short interval of 0.03 ps (thin solid line), (b) one water hydrogen atom collected over 20 ps (dashed line), and (c) the expected theoretical distribution of temperature (thick solid line). This distribution, derived from the Maxwellian velocity distribution, is given by $N(T) = N_{\text{total}}(2/\sqrt{\pi})\sqrt{(T/T_0)}\exp(-T/T_0)(\mathrm{d}T//T_0)$, where $N(T)$ is the number of observations at temperature T, N_{total} is the total number of observations, T_0 is the mean temperature (298 K), and dT is the temperature interval (25 K). The correspondence between the three distributions shows that the system is behaving ergodically and that the kinetic energy is distributed properly.

trajectory. An additional 1 ns (1000 ps) trajectory was run at 298 K to ensure the stability of the values determined over 100 ps. For all properties the values over the last 200 ps of this longer simulation were comparable to those determined during the shorter simulations.

Results and Discussion

Prior to evaluating the results of the simulation of the F3C model, it is necessary to demonstrate that the systems have reached equilibrium. This was checked by calculating the temperature, which is very sensitive and directly proportional to the kinetic energy, for each water atom as well as the translational temperature of each water molecule from the kinetic energy of the center of mass translation. In a test run averaged over the last 20 ps of a 40 ps simulation, the temperature of all water molecules was 305 K, the translational temperature was 300 K, and the temperature of the oxygen and hydrogen atoms was 301 and 308 K, respectively. These values are similar enough as to indicate a uniform temperature over the whole system. The temperature was equally stable when averaged over longer time periods, with the absolute temperature and root-mean-squared deviation being 301.7 ± 4.8 K over 200 ps and 296.7 ± 4.0 K over 1000 ps. We further tested the ergodicity of the system by comparing the distribution of temperatures of all atoms collected over a very short time (0.03 ps at 20 ps) with the corresponding distribution for any particular atom collected over a much longer time (20 ps from 20 to 40 ps). These distributions were indistinguishable and very close to the expected theoretical distribution (Figure 1). The stability and small deviation of the temperature demonstrate that equilibrium is reached in less than the 50 ps equilibration period used and that averages calculated over the next 50 ps should be unbiased.

Comparison of the F3C Model to Other Water Models and Experiment. The potential energy of the F3C model is in good agreement with experiment (within 0.2 kcal mol^{-1}, Table 2). The other three-point water models are also in reasonable agreement with experiment, with differences of 0.4−0.6 kcal mol^{-1}. Most water models have attempted to fit the experimental potential energy (derived from the heat of vaporization).[29,52,53] Consideration of the energy required to polarize a real water molecule when it goes into the liquid phase[26] indicates that the potential energy of nonpolarizable models should be corrected by about 1 kcal mol^{-1} before comparison with experiment. When this is done, the calculated potential energy that best fits experiment is close to −11 kcal mol^{-1}, and the fit to experiment of other properties is improved.[27] This correction was not made in deriving the F3C water model.

Comparison of heat capacity with experiment is more complicated due to quantum corrections.[54] The water molecules studied here are flexible: each OH bond length and HOH bond angle is a classical harmonic oscillator that absorbs (1/2)kT of kinetic energy and (1/2)kT of potential energy, for a total of 3kT for the two bonds and one angle of each water molecule, where k is Boltzmann's constant. Real water obeys quantum mechanics and is neither a flexible nor a rigid classical system. The OH bonds and HOH angles are quantum oscillators with frequencies,[54] ν, of 3455, 3345, and 1645 cm^{-1}. Using the formula for quantum mechanical heat capacity, $C_V = k\exp(h\nu/kT)[(h\nu/kT)/(\exp(h\nu/kT) - 1)]^2$ (k is Boltzmann's constant, h is Planck's constant, T is absolute temperature), gives contributions to the heat capacity of 0k, 0k and 0.03k, respectively (total 0.03k). If these vibrations were not quantized, their contribution would be 3k if flexible and 0k if rigid. The real rotational and translational degrees of water are also quantum mechanical and have characteristic frequencies of 800, 500, 500, 200, 50, and 50 cm^{-1}, giving a total contribution to the heat capacity of 4.5k. If rotational and translational modes behaved like classical oscillators, their total contribution would be 6k, and if they were like classical particles in a box, their total would be 3k. We take the correct classical value as 4.5k, the average of these values. These differences can be used to correct heat capacities calculated from classical dynamics for comparison with experimental values: for a flexible water simulation, subtract $3k + 4.5k - (0.03k + 4.5k) = 3k = 6$ cal mol^{-1} K^{-1}, and for a rigid water simulation, subtract $0k - 0.03k$ and 0 cal mol^{-1} K^{-1}. Such corrections are sometimes done in the original papers cited in Table 2, and we have not corrected values presented by others. For the F3C model, the corrected value of the heat capacity is 26 − 6 = 20 cal mol^{-1} K^{-1} (Table 2), while the experimental value is 18 cal mol^{-1} K^{-1} (see both Table 2 and Table 5 for details). We note, however, that C_V is very sensitive to the integration time step and other simulation protocols, and we merely provide C_V because it is traditionally reported for water models.

A water model for use in MD simulations should be able to reproduce the dynamic properties of water. The diffusion constant is a very important parameter because it is one of the few time dependent properties that can be measured directly, both in experiments and in simulations. And, given that transport properties are intimately related to the short- and long-range intermolecular potential,[55] diffusion provides a particularly valuable and fundamental test for a solvent model. The diffusion constant determined with F3C is in agreement with experiment (Table 2).[56]

Another experimentally measured dynamic property is the orientational correlation time, τ_2.[57,58] This single molecule autocorrelation function is defined as $\tau_{k,\alpha} = \int_0^\infty \langle P_k(e_\alpha(t)\, e_\alpha(0))\rangle\, \mathrm{d}t$, where P_k is the Legendre polynomial of order k and $e_\alpha(t)$ is a vector defining some aspect of the molecule determined at time t. The orientational correlation time, τ_2, is calculated from the second Legendre polynomial of the cosine of the angle between the HOH bisecting vector, $\theta(t)$, at time t and at time $t + \mathrm{d}t$; thus $\tau_2 = \int_0^\infty \langle {}^3/_2 \cos^2\theta(t) - {}^1/_2\rangle\, \mathrm{d}t$. We determined the value of τ_2 from a single-exponential fit to the autocorrelation function over the last 100 ps of the 1 ns simulation at 298 K. The F3C model predicted τ_2 to be 2.5 ps at 298 K, in good agreement with the experimental value of 2.4 ps[57] and in reasonable agreement with other water models.[12,58,59]

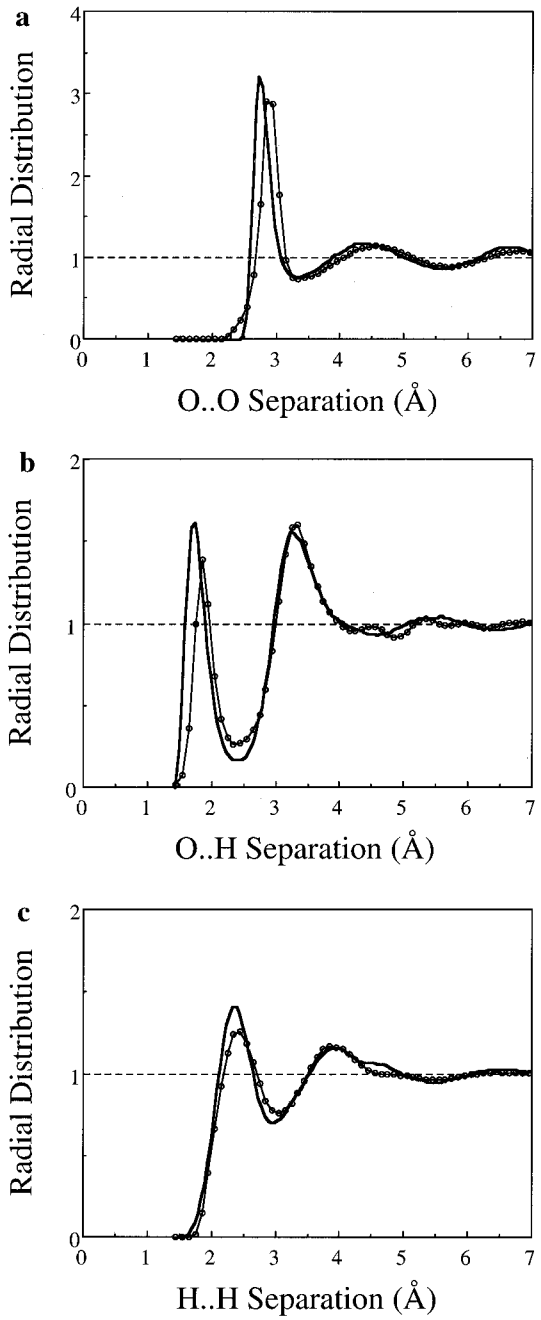

Figure 2. Water radial distribution function at 298 K simulated with a 9 Å range ($r_c = 7$ Å, solid line) is compared with the experimental curves[61] (thin line with filled circles) for (a) $g_{O\cdots O}(r)$, (b) $g_{O\cdots H}(r)$, and (c) $g_{H\cdots H}(r)$.

A good model must also reproduce the water structure determined experimentally by X-ray and neutron diffraction studies. Figure 2a shows the radial distribution function (RDF), the distribution of the interoxygen distances in any direction from a central water molecule, for the F3C model at 298 K. The positions of the peaks and valleys of the RDF are tabulated in Table 2. The first peak at 2.8 Å corresponds to two hydrogen-bonding water molecules. The second peak relates to the tetrahedral structure of near neighbors and corresponds to the oxygen−oxygen distance between two water molecules that are both hydrogen bonded to a third water molecule. Another peak around 7 Å is also evident in Figure 2a. The F3C model reproduces the overall features of the experimentally derived O···H and H···H RDF curves (Figure 2b,c).

Closer inspection of the RDFs indicates that the first peaks of all distributions are predicted to occur at too small a separation. The discrepancy in the H···H peak suggests that either the F3C OH bond length or HOH bond angle is too small (our mean values in solution are 1.04 Å and 106°, respectively). The discrepancy in the O···O and O···H peaks suggests that the F3C model gives a hydrogen bond that is 0.15 Å too short. However, testing of a modified model with a longer OH bond and larger HOH angle demonstrated that the relationship between interatomic distributions and the internal parameters is not so simple.[60] The first peak of the resulting O···O distribution function for the modified model moves only 0.05 Å closer to the experimental value, with accentuation of the height and depth of each peak or valley (data not shown). The first peaks of the O···H and H···H distributions shifted to even shorter separations, with the second peaks shifted to larger separations, in opposition to the desired changes. Additionally, the diffusion rates for this modified model dropped by approximately 50% across a range of temperatures (0.102 Å^2 ps^{-1} at 298 K and 0.226 Å^2 ps^{-1} at 348 K).

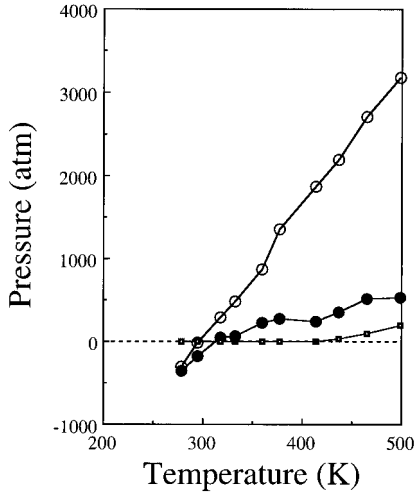

Figure 3. Simulated pressure as a function of temperature for (a) density fixed at 1.00 g/mL (open circles) and (b) density set to the value measured experimentally for water at each temperature (solid circles). If the density is not adjusted as the temperature increases, constant volume simulations like those done here can lead to very large pressures as temperature is increased. When the density is adjusted, the pressure changes are much smaller (solid circles) and in better agreement with the experimentally observed pressures at each temperature and density (solid squares).

It is interesting that early disagreement with simulations led experimentalists to re-evaluate procedures for deducing the O···O radial distribution function from neutron scattering data.[61] In particular, the experimental value[62] for the height of the first peak was 2.3, which was consistently less than the values obtained by all simulations. The newly derived peak height is now larger at 2.9 and in better agreement with simulation.

Given the recent interest in polarizable water models and the expectation that they will better model experiment than simple models, we compare the properties of these models with the simpler models (Table 2). The fit of these more complicated models is not significantly better than the simpler models, and in some cases there are severe shortcomings (for example, the PSPC model has poor O···O structure[12] and the diffusion constant of the NEMO model is too low by a factor of 3[13]). We do not mean to imply that polarization can be neglected and are sure that with better calibration these more complicated models will improve. For the present, we believe that fully tested simple models, well-calibrated to implicitly approximate some of the effects of polarizability, provide sufficiently reliable and effective potentials that fit a wide range of experimental properties without the added computational cost.

TABLE 3: Effect of Varying Temperature and Density of F3C Water[a]

		thermodynamic[b]			kinetic	structural					
						g_{OO} heights			positions (Å)		
T_{sec}[c] (K)	ρ_{set}[d] (gm cm^{-3})	T (K)	U_{pot} (kcal mol^{-1})	C_V (cal mol^{-1} K^{-1})	$D \times 10^4$ (cm^2 s^{-1})	gp1	gv1	gp2[e]	Rp1	Rv1	Rp2
273	0.999	275	−10.0	26	0.16	3.51	0.74	1.09	2.7	3.2	4.5
298	0.997	294	−9.7	26	0.24	3.31	0.80	1.07	2.8	3.3	4.6
323	0.988	317	−9.3	27	0.32	3.13	0.88		2.8	3.4	
348	0.975	333	−9.0	25	0.42	3.00	0.89		2.8	3.4	
373	0.958	358	−8.5	22	0.66	2.82	0.92		2.8	3.6	
398	0.939	378	−8.2	22	0.71	2.74	0.91		2.8	3.8	
423	0.916	414	−7.7	23	0.98	2.57	0.91		2.8	3.8	
448	0.890	437	−7.2	22	1.24	2.48	0.91		2.8	3.8	
473	0.861	468	−6.8	21	1.61	2.40	0.91		2.8	4.0	
498	0.829	499	−6.2	21	1.91	2.36	0.92		2.9	3.9	
573	0.717	582	−4.9	19	3.38	2.20	0.90		2.8	4.0	

[a] All simulations are run on a box of 216 water molecules for 100 ps with a time step of 2 fs and a range of 8 Å (cutoff of 6 Å). Averages are calculated over the last 50 ps. [b] The key to properties is given in the footnotes to Table 2. Uncorrected C_V are given. [c] T_{set} is the temperature set as the target for the equilibration procedure. After the initial equilibration, this temperature remains fixed, explaining the small differences between T_{set} and the temperature, T, calculated from the kinetic energy. [d] ρ_{set} is the set density of water in the simulation. This is the experimentally observed density of liquid water[50,51] at T_{set}. [e] No significant second peak is seen for simulations runs at or above $T_{set} = 323$ K.

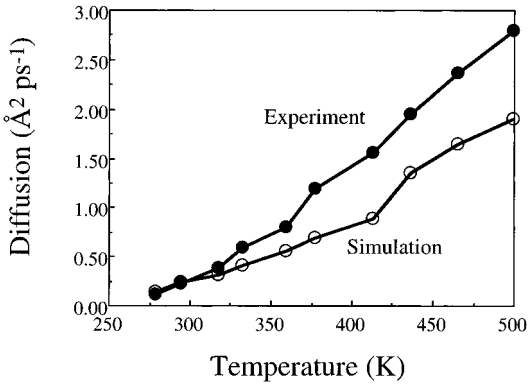

Figure 4. Variation of diffusion coefficient with temperature. The calculated diffusion rate (open circles) is about 30% smaller than the experimental values[56] (solid circles) at high temperatures. Overall the fit to experiment is good: many models have rates that are too large by a factor of 2 at room temperature.

An important aim of our macromolecular simulations is to investigate how protein structure and dynamics are affected by non-native conditions, such as extremes of temperature. Because of the importance of water in determining the properties of proteins, it is imperative to demonstrate that the water model itself reproduces the experimentally observed dependence of water properties on temperature and density changes. When the temperature is increased with the density fixed at the room-temperature value, the presssure increases steeply (Figure 3). This increase is unacceptable, particularly for thermal denaturation studies of proteins where both pressure and temperature can disrupt structure. As the temperature is increased, it is necessary to adjust the density to ensure that the pressure remains reasonable. In our work on peptides and proteins[63−67] we initially adjust the box size to yield the experimental density of liquid water for the temperature of interest. Here, we investigate the properties of pure water under these conditions. Figure 3 demonstrates that setting the density to the experimental value[50,51] at each temperature does indeed relieve most of the excess pressure. Therefore, if our simulations were run at constant pressure rather than constant volume, the density would change by only 1−2% from the experimental value.

Table 3 presents a range of water properties as a function of temperature and density. The calculated diffusion constants fit the experimental values[56] fairly well over the full temperature range (Figure 4), although the calculated value is too small at higher temperatures. Part of this disagreement arises from the higher pressure in the simulation, but it suggests that there is room for further improvement. The slowing of the dynamic process, expressed in the underestimated diffusion constant with temperature, could be related to the increased dipole moment, "which can energetically couple more strongly to the surroundings",[59] and radius of gyration of the molecule, "thus contributing to the retardation of the dynamics process".[59] Nevertheless, comparison of simulated and experimental diffusion rates over such a wide range of temperatures is unusual (and challenging for most water models at 298 K, Table 2) and provides a severe test for water models.

The water structure is also affected by increasing temperature (Table 3). As temperature increases, the first valley and second peak quickly approach a value of 1, indicative of no structure. The height of the first peak also drops but remains above 2, indicating that there is significant first-neighbor structure even at the highest temperatures. Thus, at high temperature the short-range structure due to direct hydrogen-bonding interactions is maintained, whereas the longer range structure is lost. This is shown more clearly in the various radial distribution functions given at three temperatures in Figure 5.

Recent experimental studies by Postorino et al.[68] and Tromp et al.[69] make direct comparison of high-temperature simulations of F3C with experiment possible for conditions above the boiling point of water. The radial distribution functions for the coexistence curves for F3C water at 298, 423, and 573 K (Figure 6) show favorable comparisons with the RDF curves presented in Postorino et al.[68] The loss in structure observed as the temperature is increased (shown by the decrease in peak heights and valley depths) is seen in the O···O, O···H, and H···H distribution functions. The isothermal curves showing the effect of different pressures using the F3C model also show agreement with experiment at 423 K, with the increase in pressure leading to accentuation of the peak heights and valley depths for all three distribution functions. At 573 K, the simulation shows less loss of structure at low pressure than seen in experiment;[68] thus the consequence of a pressure change is less evident in this simulation.

Stability of the F3C Model to Variations of the Simulation Protocols. Simulations of macromolecules in solution employ large boxes containing thousands of water molecules. Table 4 shows the effect of changing the number of water molecules, and hence the box size, on the calculated properties of liquid water. The calculated properties show no significant dependence on the size of the system, which varies from 54 to 1774 water molecules. In particular, it is interesting that the diffusion

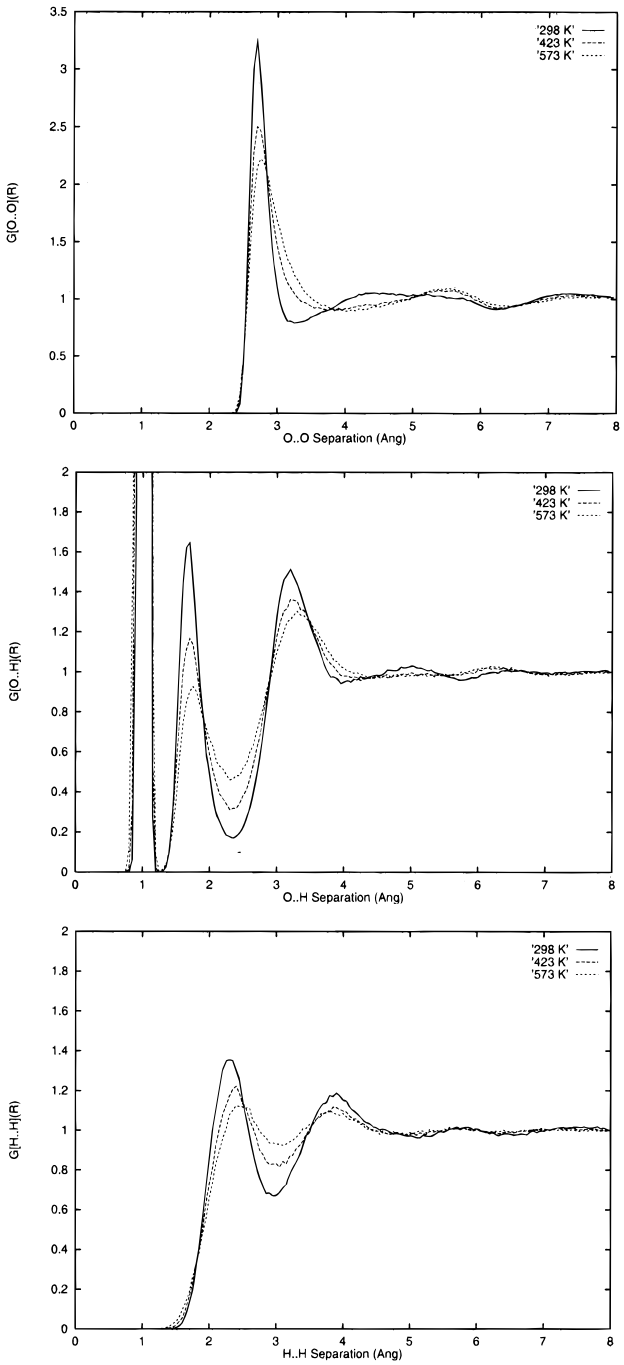

Figure 5. Variation of the O···O, O···H, and H···H RDFs as a function of temperature; 298, 423, and 573 K. For O···O, the height of the first peak is a slow function of temperature, whereas the depth of the first valley and the height of the second peak are much more affected. These simulations done with a 8 Å range (r_c = 6 Å) show a little spurious structure between 5 and 6 Å.

constant is insensitive to the box size, demonstrating that the minimum image conventions succeed in making a small finite system behave as if it were infinite.

Simulations of macromolecules in solution must be performed on the multi-nanosecond time scale to study biologically relevant processes and also to adequately sample the complicated conformational spaces of these large molecules. The simulation time for given computational resources depends directly on the integration time step Δt, thus making it important to use the largest time step consistent with energy conservation. Table 5 presents the variation of some key water properties with integration time step. The total energy is well-conserved for all time steps tested with the ratio of total energy fluctuation to kinetic energy fluctuation below 8% and the drift in total energy below 6 kcal mol^{-1} per 100 ps. The fluctuation of the total energy varies quadratically with time step, as expected for correct integration of the equations of motion. The drift also increases with time step. Although energy conservation is better with a smaller time step, all properties presented are relatively insensitive to a time step of up to 2 fs. Attempts to use time steps larger than 2 fs generally lead to a catastrophic increase in total energy and have not been pursued.

While the energy conservation is better for short time steps (Table 5), the value obtained with a 2 fs time step is better than might be expected for a flexible water model. This effect is due to the softer force constant used for the O−H bond-stretching (see Table 1), which gives an OH-stretching frequency of 2400 cm^{-1}, 30% less than the experimental value of 3400 cm^{-1}. Because our water potential is designed for simulation of macromolecules in solution, we have chosen to speed up the simulation at the expense of a more accurate representation of O−H bond vibration. Test runs with a more realistic O−H force constant (500 kcal mol^{-1} Å^{-1}) and a correspondingly shorter time step produced similar results, however (data not shown).

Calculations on macromolecules in solution need to be efficient, and this means neglecting the long-range van der Waals and Coulomb interactions beyond some range. However such cutoffs can have an adverse effect on the calculated properties.[45,46] For example, we have found that as the cutoff distance is decreased, the pressure increases, spoiling the fit to experiment. This happens because the truncated interactions are attractive, and as they are eliminated, repulsion dominates to give large excess pressures. This problem is a general one and will occur for all water models. Here, we use a single parameter to reduce repulsion, multiplying the repulsive van der Waals energy parameter $A = \epsilon r_0^{12}$ by a scale factor, A_{sc}. With the proper A_{sc} value, the fit of our model to experiment is reasonable at cutoff distances extending from 6 to 10 Å (Tables 6 and 7).

The O···O radial distribution is affected by the cutoff distance, leading to a small increase in the $g_{O\cdots O}(r)$ value at ∼0.5 Å below the cutoff distance (Figure 7). This effect is most noticeable for a 7 Å cutoff and leads to an artificially high peak between 6 and 7 Å. Thus, although we have made considerable effort to truncate energy and forces smoothly,[2] there are still small fictitious forces below the cutoff distance. The fit to experiment will always be improved by a longer cutoff at the expense of longer calculation times.

Electrostatic Screening Properties of the F3C Model. The present water model has been developed for representation of liquid water at the expense of its fit to the properties of water in the vapor phase. In liquid water, the water molecule is polarized by the electric field of the surrounding water molecules, leading to a dipole moment in solution (2.4 D) that is considerably higher than in the vapor phase (1.8 D). In rigid water models, the dipole moment remains unchanged on vaporization and the fit to the vapor properties will be poor.[27,70] In our flexible water model, the mean value of the HOH bond angle, θ^{HOH}, increases from 106.4° in solution to 109.5° *in vacuo*. The corresponding values of the OH bond length, b^{OH}, are 1.04 and 1.00 Å. On transfer to vapor, the water dipole changes by a factor of (cos(109.5°/2)/[1.04 cos(106.4°/2)] =) 0.92, to give 2.20 D *in vacuo*. Thus, the F3C flexible water model implicitly accounts for some of the effects of polarization without explicit inclusion of polarizability. Conceptually, as the electric field experienced by the water molecule increases, the OH bond length stretches and the HOH bond angle decreases

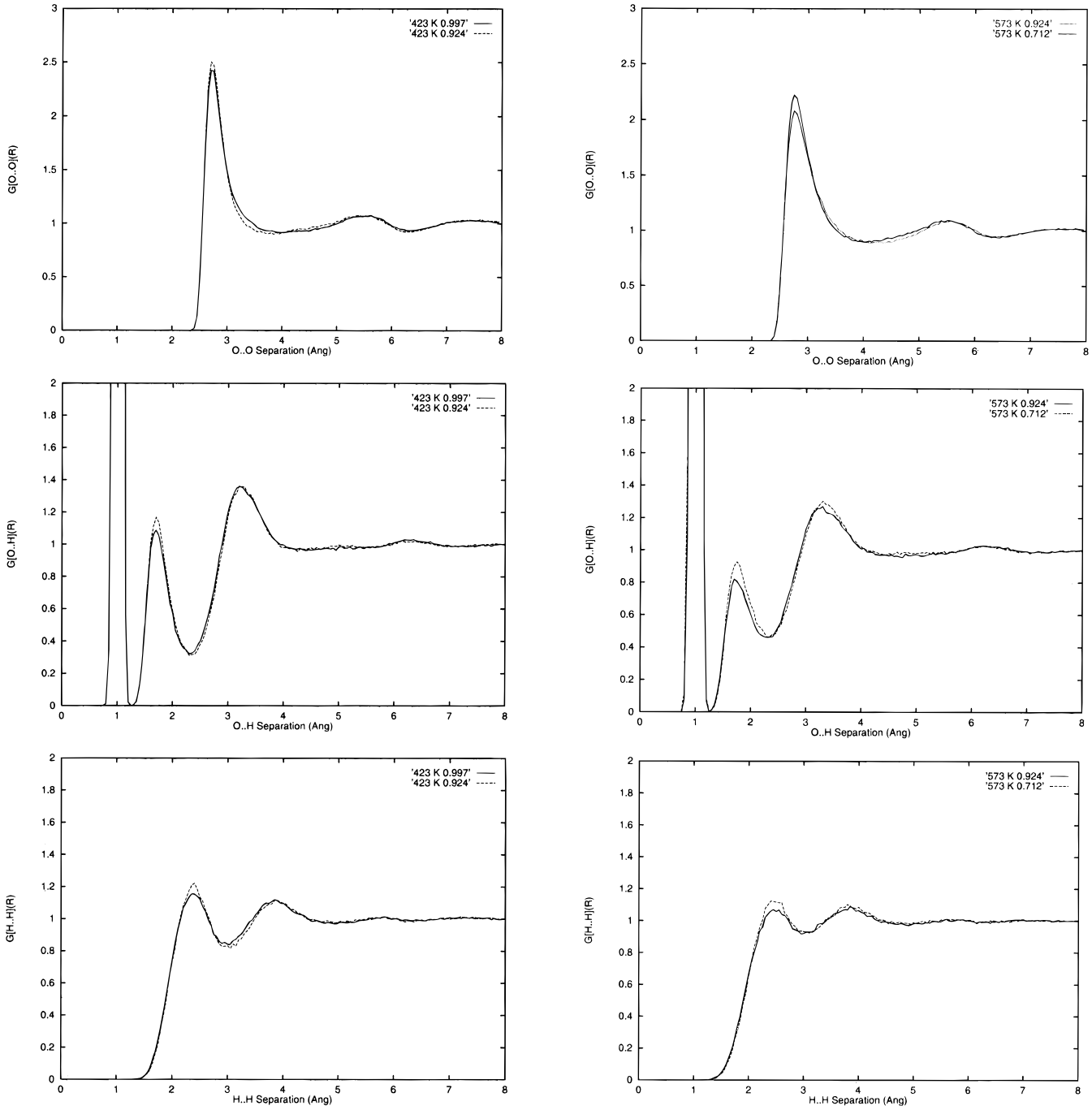

Figure 6. Effect of pressure change upon the O···O (top), O···H (middle), and H···H (bottom) RDFs at 423 (left) and 573 K (right) for comparison with experiment. The curves are labeled by temperature (K) and densities (g cm^{-3}), respectively. The curves labeled '423 K 0.924', '423 K 0.997', '573 K 0.924', and '573 K 0.712' are conditions A, B, C, and D of Postorino et al.[68]

in value to give a larger dipole moment. A general discussion of how internal flexibility mimics polarizability has been given by Dinur.[71]

A major concern for a water model that does not explicitly include polarizability is whether it can adequately screen electrostatic interactions. In simulations of solvated macromolecules, sodium or chloride counterions are often introduced to neutralize net charges arising from the ionized groups of the peptide, protein, or DNA. These counterions carry full charges, and if electrostatic interactions are not sufficiently screened by the water, there will be large disruptive forces or these counterions will become attached to a complementary charge and fail to show the proper diffusive behavior. Simulation of NaCl in water demonstrates that the screening is strong enough that the ions separate (Figure 8). Such screening also allows negatively charged chloride ions to interact favorably at a separation distance of 5 Å. At this separation, the positively charged protons of a water molecule bridge the two Cl^- ions and hold them together. The corresponding interaction of Na^+···Na^+ is weaker, probably due to their smaller size. These effects, which are counterintuitive, have also been seen in more extensive studies of ion solvation by Dang et al.[72] The existence of such seemingly unfavorable interactions suggests that the F3C model screens electrostatic interactions adequately. We also find that these ions behave similarly in simulations with cutoff distances of 6−10 Å (with the appropriate A_{sc} values, data not shown), suggesting that the short-range interactions are sufficient to provide electrostatic screening of ion···ion interactions.

TABLE 4: Effect of the Box Size on the Simulated Properties of F3C Water

		thermodynamic[a]			kinetic	structural					
						g_{OO} heights			positions (Å)		
N_{wat}[b]	side[c] (Å)	T (K)	U_{pot} (kcal mol^{-1})	C_V (cal mol^{-1} K^{-1})	$D \times 10^4$ (cm^2 s^{-1})	gp1	gv1	gp2	Rp1	Rv1	Rp2
54	11.74	304	−9.7	24	0.20	3.31	0.80	1.09	2.8	3.3	4.6
104	14.60	302	−9.6	27	0.27	3.22	0.83	1.07	2.8	3.4	4.4
159	16.82	301	−9.6	24	0.23	3.28	0.82	1.07	2.8	3.3	5.1
216	18.64	294	−9.7	26	0.24	3.31	0.80	1.07	2.8	3.3	4.6
304	20.88	296	−9.6	26	0.23	3.31	0.81	1.07	2.8	3.3	4.5
434	23.52	296	−9.6	24	0.25	3.30	0.82	1.06	2.8	3.3	4.5
864	29.58	294	−9.7	25	0.22	3.35	0.80	1.07	2.8	3.3	4.4
1774	37.60	295	−9.6	26	0.24	3.31	0.81	1.07	2.8	3.3	4.4

[a] The key to the properties is given in the footnotes to Table 2. Uncorrected C_V are given. [b] N_{wat} is the number of water molecules in the cubic box of side given above. In each case the density of the water in the box is set to 0.997 g cm^{-3} and the temperature set to 298 K. [c] The 8 Å range (6 Å cutoff) is used for all simulations even when this means violating minimum image boundary conditions (the cutoff is larger than half the box side).

TABLE 5: Effect of the Integration Time Step[a] on Simulated Properties of F3C Water

	energy		thermodynamic[b]			kinetic	structural					
							g_{OO} heights			positions (Å)		
time step (fs)	fluct.[c] ratio (%)	drift[d]/100 ps (kcal)	T (K)	U_{pot} (kcal mol^{-1})	C_V[e] (cal mol^{-1} K^{-1})	$D \times 10^4$ (cm^2 s^{-1})	gp1	gv1	gp2	Rp1	Rv1	Rp2
0.25	0.12	0.01	302	−9.6	24	0.25	3.25	0.86	1.07	2.8	3.3	4.5
0.5	0.37	0.5	303	−9.6	28	0.30	3.17	0.88	1.05	2.8	3.3	5.2
1.0	1.82	1.7	297	−9.7	28	0.24	3.28	0.85	1.07	2.8	3.3	4.5
2.0	8.69	6.1	299	−9.7	27	0.21	3.31	0.83	1.07	2.8	3.3	4.5

[a] The integration time step is given in units of 10^{-15} s (femtoseconds or fs). Each simulation was run for 100 000 time steps with the density of the water set to 0.997 g cm^{-3} and the temperature set to 298 K. [b] The key to the properties is given in the footnotes to Table 2. Uncorrected C_V are given. [c] Fluct. ratio is the ratio of the fluctuation in total energy to the fluctuation in kinetic energy expressed as a percentage. [d] Drift/100 ps is the change in average total energy (in kcal mol^{-1}) over a 100 ps time interval. [e] The accuracy of C_V is particularly sensitive to the time step used in the integration of the equations of motion. In the present work, the ratio of the fluctuation in the kinetic and in the potential energies, both possible properties from which to calculate C_V,[48] is 1.01 with a 2 fs time step, 1.00 with a 1 fs time step, and 1.00 with a 0.5 fs time step, demonstrating that the 2 fs time step is sufficient to yield consistency to within 1% for C_V.

TABLE 6: Effect of the Cutoff[a] Distance and *A*-Parameter Scale (A_{sc}) on F3C Water

		thermodynamic[c]		kinetic	structural					
					g_{OO} heights			positions (Å)		
cutoff (Å)	A_{sc}	U_{pot} (kcal mol^{-1})	C_V (cal mol^{-1} K^{-1})	$D \times 10^4$ (cm^2 s^{-1})	gp1	gv1	gp2	Rp1	Rv1	Rp2
6.0	0.84	−9.7	26	0.24	3.31	0.80	1.07	2.8	3.3	4.6
6.0	0.85	−9.5	29	0.22	3.19	0.82	1.07	2.8	3.3	4.4
6.0	0.90	−10.1	23	0.15	3.42	0.73	1.11	2.8	3.3	4.5
7.0	0.89	−9.8	26	0.17	3.28	0.72	1.19	2.8	3.3	4.4
7.0	0.90	−9.7	24	0.15	3.29	0.73	1.19	2.8	3.3	4.4
7.0	0.91	−9.6	24	0.21	3.21	0.75	1.18	2.8	3.3	4.3
9.0	0.90	−9.9	24	0.24	3.21	0.77	1.13	2.8	3.3	4.5
9.0	0.92	−9.8	25	0.23	3.11	0.82	1.10	2.8	3.3	4.3
9.0	0.94	−9.6	24	0.22	3.05	0.84	1.10	2.8	3.4	4.5
10.0	0.96	−9.9	21	0.22	3.11	0.83	1.12	2.9	3.3	4.4
10.0	1.00	−9.5	26	0.27	3.04	0.89	1.08	2.8	3.4	4.3

[a] The cutoff distance is varied from 6 to 10 Å (range of 8−12 Å), and several *A*-parameter scales are used for each distance in order to find the A_{sc} value that gives a pressure closest to zero. [b] All runs are at a set temperature of 298 K and at a set density of 0.997 g cm^{-3}. [c] The key to the properties is given in the footnotes to Table 2. Uncorrected C_V are given.

Conclusions

We have presented a flexible three-center water model (F3C) that is well-suited to simulation of macromolecules in solution. This model has been tested and found to perform very well compared to both experimental results and other models. In addition, the F3C model was simulated at a range of temperature and pressures, yielding results in agreement with experiment; such systematic comparison has not been made for other water models. We have taken a pragmatic approach and focused upon a model that reproduces both structural and dynamic behavior of water using short cutoffs and large time steps in order to make longer simulations of macromolecules in water possible. Overall, the fit of so simple a model to such a wide range of experimental properties is encouraging and bodes well for the application of the F3C model in a wide range of macromolecular simulations.

We have shown that simulations, using short cutoff distances are in good agreement with experiment, as observed previously,[73] but that a better fit to the tail of the O···O radial distribution is obtained with longer ranges. The other properties of the model are insensitive to cutoff provided the van der Waals repulsive parameter is properly scaled. Thus, our model can be used immediately with longer cutoffs as computers become faster. For macromolecules in solution, we believe there will always be the need to use the shortest possible cutoff to increase simulation time and provide better sampling for these complicated systems.

Systematic tests of the F3C model show that while the size of the system and the integration time step have little effect on

TABLE 7: *A*-Parameter Scale (A_{sc}) Appropriate for Different Cutoff Distances

		thermodynamic[a]		kinetic	structural					
					g_{OO} heights			positions (Å)		
cutoff (Å)	A_{sc}	U_{pot} (kcal mol^{-1})	C_V (cal mol^{-1} K^{-1})	$D \times 10^4$ (cm^2 s^{-1})	gp1	gv1	gp2	Rp1	Rv1	Rp2
8.0	0.84	−9.7	26	0.24	3.31	0.80	1.07	2.8	3.3	4.6
9.0	0.90	−9.7	24		3.29	0.73	1.19	2.8	3.3	4.4
10.0	0.92	−9.8	25	0.23	3.11	0.82	1.10	2.8	3.3	4.3
12.0	0.96	−9.9	21	0.22	3.11	0.83	1.12	2.9	3.3	4.4

[a] The key to the properties is given in the footnotes to Table 2. Uncorrected C_V are given.

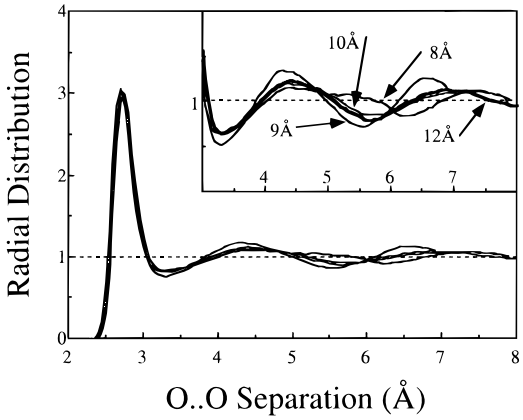

Figure 7. Effect of range on $g_{O\cdots O}(r)$. The structure of liquid water beyond the second peak in the distribution is affected by the range with a small increase in the $g_{O\cdots O}(r)$ value at about 2.5 Å below the buffer range. Note that the cutoff distance, r_c, is 2 Å less than the range value.

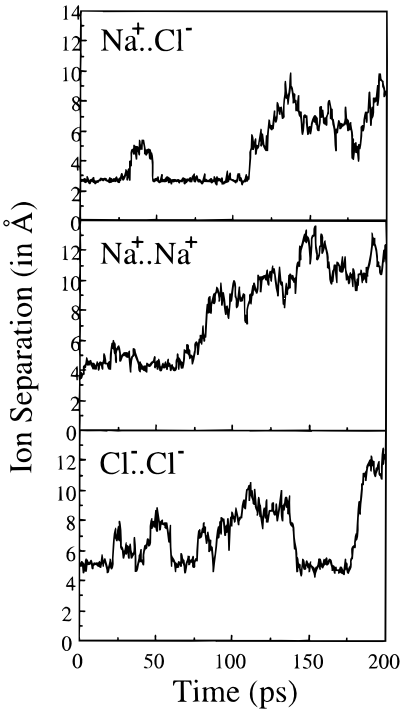

Figure 8. Dynamics of Na^+ and Cl^- ion-pairs in water. Simulating the motion of two ions in a box of 214 water molecules for 200 ps reveals differences in behavior of $Na^+\cdots Cl^-$, $Na^+\cdots Na^+$, and $Cl^-\cdots Cl^-$. In all cases the ions start in close contact. The panels give the variation with time of the ion separation. From this it is clear that $Na^+\cdots Cl^-$ interact strongly at 2.7 Å and less strongly, but significantly, at 4.7 Å. $Na^+\cdots Na^+$ interact weakly at 4.3 Å; once broken this interaction does not reform. $Cl^-\cdots Cl^-$ interact more strongly at 5 Å; this interaction is stable and reformed easily.

liquid properties of water, the method of truncation of the longer range terms of the potential is crucial for the accurate representation of the system. Without smooth and gradual truncation of the long-range van der Waals and electrostatic interactions, the total energy is not conserved, the diffusion of water molecules is unrealistically fast,[74] and the second peak in the oxygen−oxygen radial distribution function (a measure of tetrahedral structure) is absent. The factors leading to our improved dynamic properties are (a) consistent parametrization of a flexible three-atom model, (b) smooth truncation of nonbonded interactions, (c) conservation of energy in a NVE ensemble, (d) use of a weaker OH bond force constant for more efficient dynamics, and (e) scaling of the repulsive van der Waals energy. These features of our water potential are consistent with potentials generally used for macromolecules. It is this consistency that makes it possible to use the F3C model for multi-nanosecond simulation of macromolecules in solution over a wide range of temperatures and densities.

Acknowledgment. We thank Mark Gerstein for constructive criticism of the manuscript. This work was supported by the National Institutes of Health (GM41455 to M.L.), the National Science Foundation (DMB8720208 to M.L.) and the Office of Naval Research (N00014-95-0484 to V.D.).

References and Notes

(1) Levitt, M. *J. Mol. Biol.* **1983**, *168*, 595.
(2) Levitt, M.; Hirshberg, M.; Sharon, R.; Daggett, V. *Comput. Phys. Commun.* **1995**, *91*, 215.
(3) Levitt, M.; Sharon, R. *Proc. Natl. Acad. Sci. U.S.A.* **1988**, *85*, 7557.
(4) Daggett, V.; Kollman, P.; Kuntz, I. D. *Biopolymers* **1991**, *31*, 285.
(5) Lifson, S. *J. Chim. Phys.* **1968**, *65*, 40.
(6) Levitt, M.; Lifson, S. *J. Mol. Biol.* **1969**, *46*, 269.
(7) Levitt, M. *J. Mol. Biol.* **1974**, *82*, 393.
(8) Rahman, A.; Stillinger, F. H. *J. Chem. Phys.* **1971**, *55*, 3336.
(9) Howard, A. E.; Singh, U. C.; Billeter, M.; Kollman, P. A. *J. Am. Chem. Soc.* **1988**, *110*, 6984.
(10) Sprik, M.; Klein, M. L. *J. Chem. Phys.* **1988**, *89*, 7556.
(11) Watanabe, K.; Klein, M. L. *Chem. Phys.* **1989**, *131*, 2.
(12) Ahlstrom, P.; Wallqvist, A.; Engstrom, S.; Jonsson, B. *Mol. Phys.* **1989**, *68*, 563.
(13) Caldwell, J.; Dang, L. X.; Kollman, P. A. *J. Am. Chem. Soc.* **1990**, *112*, 9144.
(14) Wallqvist, A.; Ahlstrom, P.; Karlstrom, G. *J. Phys. Chem.* **1990**, *94*, 1649.
(15) Kuwajima, S.; Warshel, A. *J. Phys. Chem.* **1990**, *94*, 460.
(16) Zhu, S. B.; Surjit, S.; Robinson, G. W. *J. Chem. Phys.* **1991**, *95*, 2791.
(17) Wallqvist, A. *Chem. Phys.* **1991**, *148*, 439.
(18) Dang, L. X. *J. Chem. Phys.* **1992**, *97*, 2659.
(19) van Belle, D.; Froeyen, M.; Lippens, G.; Wodak, S. J. *Mol. Phys.* **1992**, *77*, 239.
(20) Wallqvist, A.; Astrand, P. O. *J. Chem. Phys.* **1995**, *102*, 6559.
(21) Rossky, P. J.; Karplus, M. *Biopolymers* **1979**, *18*, 825.
(22) Berendsen, H. J. C.; Postma, J. P. M.; van Gunsteren, W. F.; Hermans, J. *Intermolecular Forces*; Pullmann, B., Ed.; Reidel: Dordrecht, The Netherlands, 1981; Vol. B14, p 331.
(23) Jorgensen, W. L. *J. Am. Chem. Soc.* **1981**, *103*, 335.
(24) Lifson, S.; Warshel, A. *J. Chem. Phys.* **1968**, *49*, 5116.
(25) Warshel, A.; Lifson, S. *J. Chem. Phys.* **1970**, *53*, 582.
(26) Hagler, A. T.; Huler, E.; Lifson, S. *J. Am. Chem. Soc.* **1974**, *96*, 5319.
(27) Jorgensen, W. L.; Chandraseckhar, J.; Madura, J. D.; Impey, R. W.; Klein, M. L. *J. Chem. Phys.* **1983**, *79*, 926.
(28) Berendsen, H. J. C.; Grigera, J. R.; Straatsma, T. P. *J. Phys. Chem.* **1987**, *91*, 6269.
(29) Stillinger, F. H.; Rahman, A. *J. Chem. Phys.* **1978**, *68*, 666.

(30) Toukan, K.; Rahman, A. *Phys. Rev. B* **1985**, *31*, 2643.
(31) Teleman, O.; Ahlstrom, P. *J. Am .Chem. Soc.* **1986**, *108*, 4333.
(32) Anderson, J.; Ullo, J.; Yip, S. *J. Chem. Phys.* **1987**, *87*, 1726.
(33) Tironi, I. G.; Brunne, R. M.; van Gunsteren, W. F. *Chem. Phys. Lett.* **1996**, *250*, 19.
(34) Dang, L. X.; Pettitt, B. M. *J. Phys. Chem.* **1987**, *91*, 3349.
(35) Reimers, J. R.; Watts, R. O. *Chem. Phys.* **1984**, *91*, 201.
(36) Barrat, J. L.; McDonald, I. R. *Mol. Phys.* **1990**, *70*, 535.
(37) Smith, P. E.; Pettitt, M. B. *J. Chem. Phys.* **1995**, *95*, 8430.
(38) Ruff, I.; Diestler, D. J. *J. Chem. Phys.* **1990**, *93*, 2032.
(39) Zhu, S. B.; Robinson, G. W. *J. Chem. Phys.* **1991**, *94*, 1403.
(40) Guardia, E.; Rey, R.; Padro, J. A. *Chem. Phys.* **1991**, *155*, 187.
(41) Corongiu, G.; Clementi, E. *J. Chem. Phys.* **1992**, *97*, 2030.
(42) Sciortino, F.; Corongiu, G. *J. Chem. Phys.* **1993**, *98*, 5694.
(43) Ferguson, D. M. *J. Comput. Chem.* **1995**, *16*, 501.
(44) Lau, K. F.; Alper, H. E.; Thatcher, T. S.; Stouch, T. R. *J. Phys. Chem.* **1994**, *98*, 8785.
(45) Brooks, C. L., III; Pettit, B. M.; Karplus, M. *J. Chem. Phys.* **1985**, *83*, 5897.
(46) Feller, S. E.; Pastor, R. W.; Rojnuckarin, A.; Bogusz, S.; Brooks, B. R. *J. Phys. Chem.* **1996**, *100*, 17011.
(47) Daggett, V.; Levitt, M. *J. Mol. Biol.* **1992**, *223*, 1121.
(48) Allen, M. P.; Tildesley, D. J. *Computer Simulation of Liquids*; Clarendon Press: Oxford, 1987.
(49) Levitt, M. *ENCAD*−Energy Calculations and Dynamics; Molecular Applications Group: Stanford and Yeda, 1990.
(50) Kell, G. S. *J. Chem. Eng. Data* **1967**, *12*, 66.
(51) Haar, L.; Gallagher, J. S.; Kell, G. S. *NBS/NRC steam tables*: thermodynamic and transport properties and computer programs for vapor and liquid states of water in SI units; Hemisphere Pub. Corp.: Washington, DC, 1984.
(52) Owicki, J. C.; Scheraga, H. A. *J. Am. Chem. Soc.* **1977**, *99*, 7403.
(53) Lie, G. C.; Clementi, E.; Yoshimine, M. *J. Chem. Phys.* **1976**, *64*, 2314.
(54) Eisenberg, D.; Kauzmann, W. *The Structure and Properties of Water*; Oxford University Press: Oxford, 1969.
(55) Tyrell, H. J. V.; Harris, K. M. *Diffusion in Liquids: A Theoretical and Experimental Study*; Butterworths: London, 1984.
(56) Krynicki, K.; Green, C. D.; Sawyer, D. W. *Discuss. Faraday Soc.* **1978**, *66*, 199.
(57) Halle, B.; Wennerström, H. *J. Chem. Phys.* **1981**, *75*, 1928.
(58) Svishchev, I. M.; Kusalik, P. G. *J. Phys. Chem.* **1994**, *98*, 728.
(59) Wallqvist, A.; Teleman, O. *Mol. Phys.* **1991**, *74*, 515.
(60) The OH bond length (1.15 Å) and HOH bond angle (106.47°) parameters were changed with consequential changes in the atomic charges (q(O) = −0.692e and q(H) = 0.346e) in order to maintain the correct molecular dipole moment.
(61) Soper, A. K.; Phillips, M. G. *Chem. Phys.* **1986**, *107*, 47.
(62) Narten, N. H.; Thiessen, W. E.; Blum, L. *Science* **1982**, *217*, 1033.
(63) Daggett, V.; Levitt, M. *J. Mol. Biol.* **1993**, *232*, 600.
(64) Li, A.; Daggett, V. *Proc. Natl. Acad. Sci. U.S.A.* **1994**, *91*, 10430.
(65) Alonso, D. O. V.; Daggett, V. *J. Mol. Biol.* **1995**, *247*, 501.
(66) Li, A.; Daggett, V. *J. Mol. Biol.* **1996**, *257*, 412.
(67) Laidig, K. E.; Daggett, V. *Folding Des.* **1996**, *1*, 335.
(68) Postorino, P.; Ricci, M. A.; Soper, A. K. *J. Chem. Phys.* **1994**, *101*, 4123.
(69) Tromp, R. H.; Postorino, P.; Neilson, G. W.; Ricci, M. A.; Soper, A. K. *J. Chem. Phys.* **1994**, *101*, 6210.
(70) Reimers, J. R.; Watts, R. O.; Klein, M. L. *Chem. Phys.* **1982**, *64*, 95.
(71) Dinur, U. *J. Phys. Chem.* **1990**, *94*, 5669.
(72) Dang, L. X.; Pettitt, B. M.; Rossky, P. J. *J. Chem. Phys.* **1992**, *96*, 4046.
(73) Andrea, T. A.; Swope, W. C.; Andersen, H. C. *J. Chem. Phys.* **1983**, *79*, 4576.
(74) Levitt, M. *Chem. Scr.* **1989**, *29A*, 197.
(75) Weiner, S. J.; Kollman, P. A.; Case, D. A.; Singh, U. C.; Ghio, C.; Alagona, G.; Profeta, S. J.; Weiner, P. *J. Am. Chem. Soc.* **1984**, *106*, 756.
(76) Brooks, B. R.; Bruccoleri, R. E.; Olafson, B. D.; States, D. J.; Swaminanthan, S.; Karplus, M. *J. Comput. Chem.* **1983**, *4*, 187.
(77) Benal, J. D.; Fowler, R. H. *J. Chem. Phys.* **1933**, *1*, 515.
(78) Naim, A. B.; Stillinger, F. H. *Aspects of the Statistical-Mechanical Theory of Water*; Wiley-Interscience: New York, 1971.
(79) Stillinger, F. H.; Rahman, A. *J. Chem. Phys.* **1974**, *60*, 1545.
(80) Matsuoka, O.; Clementi, E.; Yoshimine, M. *J. Chem. Phys.* **1976**, *64*, 1351.
(81) Impey, R. W.; Madden, P. A.; McDonald, I. R. *Chem. Phys. Lett.* **1982**, *88*, 589.
(82) Reddy, M. R.; Berkowitz, M. *J. Chem. Phys.* **1987**, *87*, 6682.